**Nationaal Lucht- en Ruimtevaartlaboratorium**
National Aerospace Laboratory NLR

NLR TP 97261

# Flow visualization and particle image velocimetry on a semi-span straked delta wing, stationary and oscillating in pitch

E.G.M. Geurts and A.M. Cunningham Jr.

# DOCUMENT CONTROL SHEET

| | ORIGINATOR'S REF. | | SECURITY CLASS. |
|---|---|---|---|
| | TP 97261 U | | Unclassified |

ORIGINATOR
National Aerospace Laboratory NLR, Amsterdam, The Netherlands

TITLE
Flow visualization and particle image velocimetry on a semi-span straked delta wing, stationary and oscillating in pitch

PRESENTED AT
the European Forum on Wind Tunnel Test Techniques, Cambridge, United Kingdom, April 14-16, 1997.

| AUTHORS | DATE | pp | ref |
|---|---|---|---|
| E.G.M. Geurts and A.M. Cunningham Jr. | 970509 | 15 | 8 |

DESCRIPTORS

| | |
|---|---|
| Delta wings | Transonic flow |
| Flow visualization | Vortex sheets |
| Particle image velocimetry | Water vapor |
| Semispan models | Wind tunnel tests |
| Separated flow | Wing oscillations |
| Strakes | |

ABSTRACT
The Unsteady Transonic Delta Program (UTDP), an ongoing cooperative U.S.-Dutch program of research between Lockheed Martin Tactical Aircraft Systems, Fort Worth, Texas, USA and the National Aerospace Laboratory (NLR), Amsterdam, the Netherlands, focuses on two closely related areas: Limit Cycle Oscillations (LCO) on a realistic fighter configuration and unsteady transonic flows about a Simple Straked delta wing.
As part of this program a wind tunnel visualization test on a highly instrumented semi-span straked delta wing model was conducted in NLR's High Speed Tunnel in August 1996.
Flow visualization was conducted using a vapour screen technique with multiple laser light sheet positions, highlighting flow field characteristics associated with Limit Cycle Oscillations and high incidence shock/vortex interactions and flow breakdown. After the completion of the flow visualization program an application of the non intrusive quantitative flow field measurement technique DPIV (Digital Particle Image Velocimetry) was demonstrated.
In the paper the flow visualization and PIV test techniques will be explained and results will be presented and discussed.

Contents



(15 pages in total)

This page is intentionally left blank

# FLOW VISUALIZATION AND PARTICLE IMAGE VELOCIMETRY ON A SEMI-SPAN STRAKED DELTA WING, STATIONARY AND OSCILLATING IN PITCH.

E.GM. Geurts'
National Aerospace Laboratory NLR
Amsterdam, The Netherlands

## Abstract

The Unsteady Transonic Delta Program (UTDP), an ongoing cooperative U.S.-Dutch program of research between Lockheed Martin Tactical Aircraft Systems, Fort Worth, Texas, USA and the National Aerospace Laboratory (NLR), Amsterdam, the Netherlands, focuses on two closely related areas: Limit Cycle Oscillations (LCO) on a realistic fighter configuration and unsteady transonic flows about a Simple Straked delta wing.
As part of this program a wind tunnel visualization test on a highly instrumented semi-span straked delta wing model was conducted in NLR's High Speed Tunnel in August 1996.
Flow visuaiization was conducted using a vapour screen technique with multiple laser light sheet positions, highlighting flow field characteristics associated with Limit Cycle Oscillations and high incidence shock/vortex interactions and flow breakdown. After the completion of the flow visualization program an application of the non intrusive quantitative flow field measurement technique DPIV (Digital Particle Image Velocimetry) was demonstrated.
In the paper the flow visualization and PIV test techniques will be explained and results will be presented and discussed.

## List of symbols, subscripts. abbreviations

| | | |
|---|---|---|
| alpha a | [°,deg] | mean incidence |
| dalpha da | [°,deg] | model amplitude |
| freq, f | [Hz] | frequency |
| M | r-1 | Mach number |
| phi, φ | [°,deg] | phase angle |
| Re | [-] | Reynolds number |

| | |
|---|---|
| C | camera trigger |
| m | model |

| | |
|---|---|
| HRC | High Resolution Camera |
| IHSV | Intensified High Speed Video (Camera) |
| LCO | Limit Cycle Oscillation |
| PIV | Particle Image Velocimetry |
| SiS | Simple Strake |
| UTDP | Unsteady Transonic Delta Program |

. Research Scientist
Department of Aerodynamic Engineering and Aeroelasticity

## 1 Introduction

To understand the development of aerodynamic loads for tighter aircraft manoeuvring beyond stall, a low-speed wind tunnel test was performed on a full span simple strake model at NLR in 1986 as described in reference 1.
In order to increase the understanding of the physics of unsteady vortex flows with compressibility effects and to generate an extended airloads data base for computer code evaluation a follow-up test program was considered. In addition, flight experience with various fighter aircraft showed that limited amplitude aeroelastic oscillations (LCO) at lower angles of attack presented a serious problem by imposing flight envelope restrictions. In view of the combined interest in these LCO problems and in transonic vortex flows an extensive program of research, the Unsteady Transonic Delta Program, was planned and executed. This program consisted of three parts:

- conducting an unsteady transonic wind tunnel test (LCO test) on fighter configurations at conditions typical of full-scale LCO, a limited amplitude self-sustaining oscillation produced by a structural./ aerodynamic interaction, generally occurring at (heavily) loaded fighter type wings at transonic speeds; shock induced and trailing edge separation play a dominant role in LCO development.
- development of an LCO prediction method and
- conducting an unsteady wind tunnel test on a semi-span simple suaked delta wing model, with the same planform as (half of) the mode1 as used in the test described in reference 1.

The LCO test was performed in September 1991 (Refs. 2 and 3); the Simple Strake test in May 1992 (Ref. 4). For the prediction method, which is still in development the reader is referred to references 5 and 6.
It was already obvious that it would take a significant amount of time to fully predict and solve LCO problems numerically and that for the near future it was necessary to be satisfied with an "engineering" approach, in which the existing numerical formulation had to be combined with empirical quantities, to be derived from wind tunnel testing.
However, the wind tunnel tests provided the results to completely satisfy the needs and knowledge to predict LCO only in a limited amount. Also, in the the low speed test it was experienced mat addition of flow visualization data to the measured force and pressure

data was of great importance for understanding the flow phenomena. Because of these two reasons it was decided to conduct an additional test to obtain flow-visualization data to complement the high speed unsteady force and pressure data base with spatial information.
This visualization test was funded by the U.S. Air Force, Lockheed Martin Tactical Aircraft Systems, the Dutch Ministry of Defence and NLR. Main targets were the following:

- to identify flow field characteristics for conditions typical of transonic Limit Cycle Oscillations, mainly occurring at low incidences below 12°,
- to identify flow field characteristics for conditions dominated by vortex, shock/vortex interactions and separated flows, mainly at high incidences above 12" up to post stall, and
- to determine temporal and spatial properties of these characteristics in both incidence ranges.

The visualization supports the development of algorithms to transform the wind tunnel data in empirical quantities, used in the LCO prediction method. Results of the visualization study will also form an indispensable part in the database to evaluate existing numerical methods to predict unsteady aerodynamic forces on vibrating wings.

## 2 Test Setup

### 2.1 Wind Tunnel

The UTDP visualization test was conducted in the NLR High-Speed wind Tunnel situated in Amsterdam. This HST has a closed circuit with a test section length of about 2.5 m. Top and bottom of the test section are slotted walls with an open ratio of 12 percent. The velocity range is $0 < M < 1.3$ and by changing the stagnation pressure from 12 kPa to 390 kPa a wide range of Reynolds numbers can be covered.
Data in this section refer to the state of the wind tunnel in the "old" configuration with the test section of 2.0 x 1.6 m², because that was equivalent to the situation at the time both LCO and Simple Strake tests were conducted.
In 1992 phase I of a modernization program was executed in which the test section, the model support system and the tunnel control system of the HST were replaced. Modification of the test section concerned the enlargement to 2.0 x 1.8 m², enabling the possibility to test at higher Mach numbers. Adjustment of the upper and lower walls allows operation in both configurations.
A new modification is being executed and will be completed early spring 1997. The main activity in this phase 2 of the modernization is the construction of a connection to Amsterdam's public electrical power network. The modifications result in a considerable expansion of the HST's working envelope in the Mach number versus Reynolds number plane (figure 1). The new power system leads to a substantial reduction of the operating cost of the HST, owing to lower energy and personnel costs. By shorter starting and stopping times it will also enable the HST to be run more efficiently.

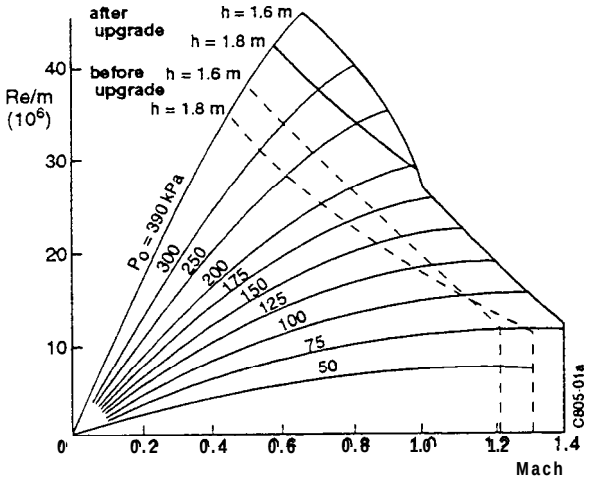


Figure 1: HST's working envelope.

### 2.2 Model, Model Support and Excitation

Because the effects governing typical transonic LCO were expected to act especially on the outboard region of the wing, where hardly any influence of fuselage shape would be noticeable, it was decided to use the Simple Strake model, but with the possibility to connect various launcher and launcher/missile combinations at the tip station.
The same highly instrumented outboard wing panel and support system were used as for the earlier test devoted to Limit Cycle Oscillation investigations. In the LCO test a fighter type fuselage was fixed to the turntable and only me outboard wing was oscillated in pitch. In the Simple Strake test, the transonic counterpart to the low-speed test (reference 1), me strake section had to move with the wing and was, therefore, attached to the basic wing panel. The Simple Strake configuration and support system is shown in figure 2.
Support was provided through a semi-span balance beam which in turn was supported by bearings mounted on the side wall turntable. The inboard part of the wing panel was thickened to accommodate the balance beam, without making contact.
Oscillatory motion of the balance beam and consequently of the model was provided by HYDRA II, an elecuo-hydraulic shaker system, which consisted of a hydraulic power supply, linear actuator and servovalve and a feedback control unit. The actuator was suspended in a box, bolted rigidly to the turntable. The piston was connected to a crank to convert the linear motion into a rotational one. Model mean angle-of-attack was controlled through positioning of the side

wall turntable.
The wing panel was of a "clam-shell" design so that all instrumentation inside the wing was accessible. It was fabricated of high-strength aluminium alloy so as to minimize inertia loads. It had instrumented flaps, whose positions could be varied, but for this test leading and trailing edge flaps were fixed at 0°. For the tip station balances were available to carry various launcher and launcher/missile combinations, all made off carbon fibre material, also to minimize inertial loads.
Loads from both the wing and strake were carried through the semi-span balance beam.
All model and support system parts were designed and fabricated by NLR. Also instrumentation and calibration were accomplished by NLR.

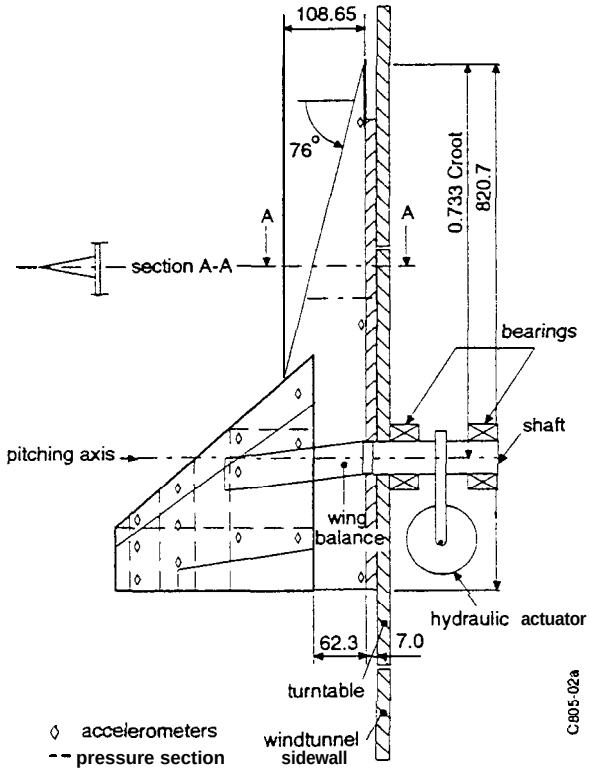


Figure 2: Simple Strake configuration and support system

## 2.3 Model Instrumentation

The model instrumentation consisted of a main wing semi-span balance, a tip launcher balance or a tip launcher/tip missile balance (depending on the choice of configuration), a dynamic incidence transducer (LVDT), in-situ pressure transducers (not used in this test), accelerometers and temperature sensors.

The three component main wing balance was designed to provide adequate stiffness and strength and yet retain sufficient sensitivity for accurate aerodynamic loads measurements. Specifically, this balance measured normal force, pitching moment and rolling (or bending) moment. The weapons at the tip were mounted on 5-component balances (tangential force excluded). To obtain optimal information two tip-balances were designed and fabricated: one balance for measuring various launcher loads (two launcher configurations possible) and one balance for measuring various launcher/missile loads (two launcher/missile configurations possible)

A linear variable differential transducer (LVDT) was mounted between the beam balance and the support to measure the oscillation amplitude input to the model. Mean incidence of the model was measured by a very sensitive accelerometer attached to the side wall turntable.

Vertical accelerometers were located at 12 positions on the wing and at 3 positions on the strake as shown in figure 2.

In the vapour screen visualization test the model was "polluted" with precipitated water droplets and during the Particle Image Velocimetry (PIV) test with precipitation of oil smoke; because the effect of these substances on the measured pressures was unknown it was decided to tape the pressure orifices.
Though pressures were not measured in this test, correlations with pressure measurements in the LCO and Simple Strake test should be possible. Therefore the laser light sheet testing was done at or very close to the four chordwise and three spanwise pressure section locations.
Grouping of the pressure sections toward the wing tip was done in order to concentrate instrumentation in the regions of known shock-induced separation as well as leading edge separation. The three spanwise rows were located for identifying shock/vortex interactions at high incidence.

## 2.4 Measurement System

The wind tunnel tests were performed using a computer controlled data acquisition system called PHARAO, Processor for HArmonic and RAndom Oscillations, which was capable of sampling 128 (time) signals simultaneously. A block diagram of the measurement system is presented in figure 3.
The electrical signals of the instruments were first amplified in the Multi-Channel Conditioning Units and a separation was made between AC (alternating current) and DC (direct current). The AC signals were filtered for anti-aliasing, sampled by the Analog Digital Convertor and stored on optical disc. One oscillator was used to control both the hydraulic actuator (see section 2.2) as well as the sampling of the electrical signals, to have perfect synchronization. Sample frequencies and filter settings were chosen proportional to the driving frequency of the model.
In most cases, for each channel 4096 samples were

recorded; the sample frequency was 128 times the model motion frequency, leading to 32 cycles.
For quick-look presentation, the time traces were averaged using Phase-Locked Time Domain Averaging (PLTDA) and Fourier-transferred to harmonic components. The balance loads were corrected for inertial loads and the influence of temperature on pressure transducer sensitivity was accounted for.

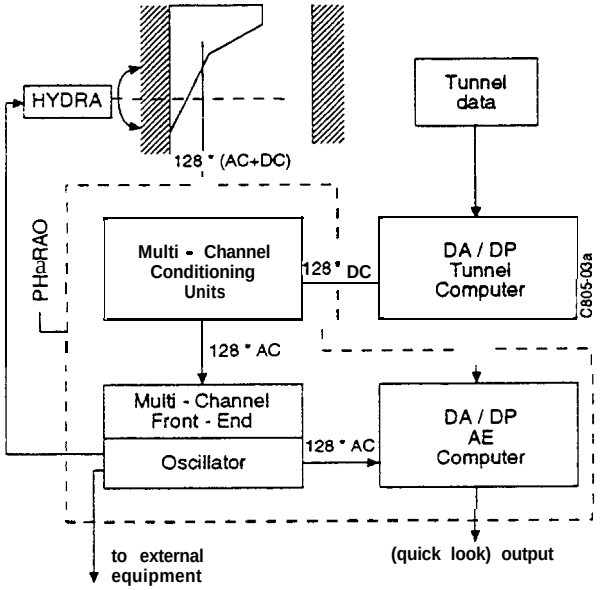


Figure 3: Measurement system as used in UTDP

## 2.5 Vapour Screen Flow Visualizadon

In figure 4 a schematic overview of the visualization test setup is presented. On the upper part a sideview of the wind tunnel test section is shown, while the lower part of the figure shows the cross-section of the HST at the model position. Three aspects must be realized for the flow visualization:

- particles in the flow,
- light to illuminate the particles, and
- registration of the pictures formed by the light, reflected by the particles.

Downstream of the test section, water is brought into the flow. Valves in the upper wail are opened during periods which are multiples of the "turn around time" in the wind tunnel, so, a good distribution of the water in the flow is obtained. No special nozzles are needed for the vaporization of the water, as was demonstrated in a preparatory test in the HST in January 1991 and in a visualization demonstration during the Simple Strake test in May 1992. By controlling the water input in the beginning of the test and the tunnel temperature and pressure during the test, the dew point can be varied in such a way, that condensation of the water starts only in expansion regions above the model.
The small droplets above the model are illuminated by a laser light sheet, formed by a 5 Watt argon ion laser and a cylindrical lens. The laser is positioned outside the plenum of the wind tunnel because it can not withstand a non-atmospheric environment. Via an optical fibre the laser light is fed into an optical system to produce the laser light sheet. This system is attached to a remotely controlled traversing mechanism, mounted on the second slat of the upper tunnel wall. It enables adjustment of the screen in either chordwise or spanwise direction. The pitch angle can be varied between about -25 to 25 degrees, enabling positioning of the (spanwise) light sheet perpendicular to the model surface at incidence. By rotating the cylindrical lens, the sheet is turned in chordwise direction with a possible rolling angle variation between -25 and +25 degrees. The range for positioning the screen in x-direction is about 2.5 meter, enabling positioning of the light screen even beyond the trailing edge of the model.

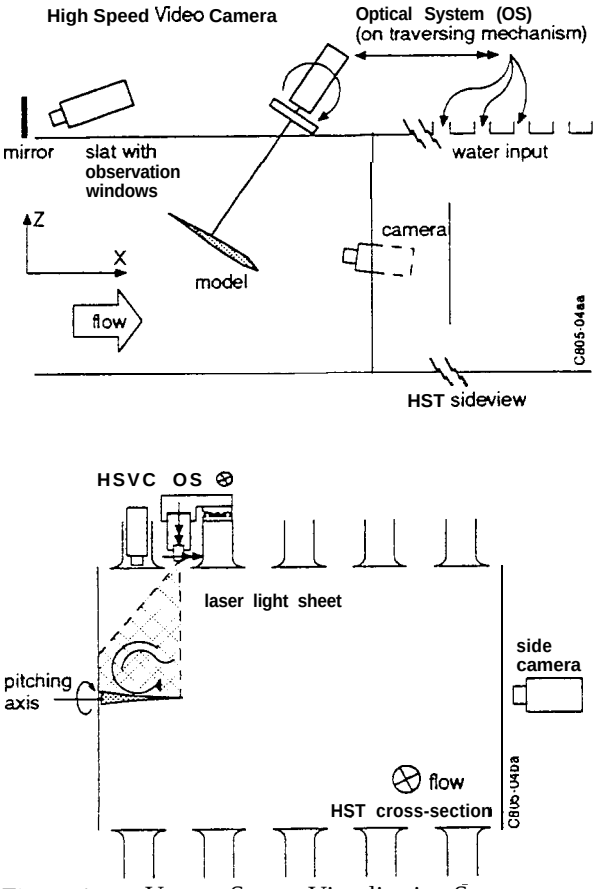


Figure 4: Vapour Screen Visualization Setup

Registration of flow phenomena at spanwise laser light sheets is done by two normal video cameras, one mounted downstream of the model on the sting support boom and the other positioned on the side wall opposite and downstream of the model. A very sensitive (about 1.5 lux) high speed video camera, is positioned in the first slat of the upper tunnel wall (see figure 4). At chordwise screen positions a normal video camera is positioned at the window in the side

wall opposite the model.
Marks were put on the model and the turntable on the upper side of the model at well-defined positions to be able to apply image-processing on the recordings made by the intensified high speed video camera to locate flow induced phenomena.

## 2.6 Particle Image Velocimetry

In figure 5 a schematic overview of the Particle Image Velocimetry test setup is presented. (For description of the PIV testing procedure the reader is referred to section 3.3). The upper part shows again a sideview and the lower part a cross view of the wind tunnel test section.

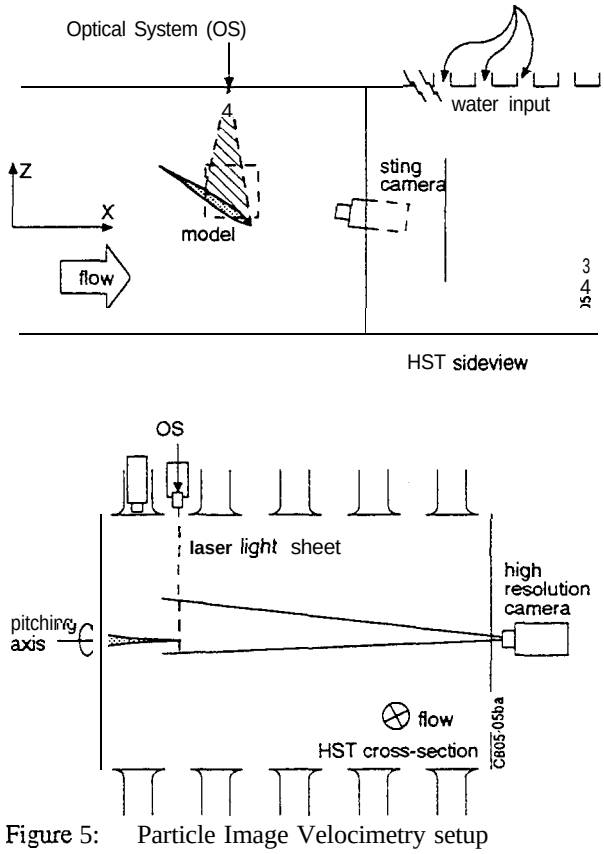


Figure 5: Particle Image Velocimetry setup

For the particles in the flow to be visualized during this demonstration use was made of oil smoke and nebulized oil. This seeding was brought in the flow in the settling chamber of the tunnel by means of a rake positioned such that the seeding reached the model at the desired location. It was also tried to apply PIV measurements using vaporized water, put in the flow at the same position as in the visualization test.
The particles above the model are illuminated by a laser light sheet, generated by a high power pulse laser and a set of mirrors and lenses fixed to the wind tunnel measurement section. Because of the complexity of such a setup, traversing of the light sheet was not possible (yet) and the demonstration was focused on only one chordwise light sheet position near the tip of the clean model configuration.
Registration of me chordwise laser light sheets was done by a high resolution camera fixed to the side wall and positioned in front of the window in the side wall opposite the model. Because the intensity of reflections on the model surface is much higher than the intensity of the light scattered by the particles in the flow, the model needed to be totally black, therefore the marks on model and turntable were eliminated.

# 3 Procedures and Measurement Techniques

The main objective of the measurements was to establish the relationship between the mechanical motion of the model as input and the forces and moments of me balances as output with simultaneous registration of the flow patterns.

## 3.1 Measurement of the balance loads

Using me data acquisition system, the relationship between model motion and balance output was established through determination of the zeroth (mean) and the first seven harmonics of the measured output signals. All data quantities were normalized into standard coefficient form using model motion and wind tunnel aerodynamic quantities for me normalization terms. The data items obtained were:

- Mean values, the first seven harmonics and time histories of all force and moment coefficients for the wing and tip loading;
- Amplitudes, derived from accelerometer signals.

With exception of the mean value quantities, all unsteady quantities were normalized with the model amplitude.

## 3.2 Vapour Screen Flow Visualization Testing

Because of the importance of flow visualization for understanding shock/vortex interactions at transonic speeds, additional testing with the vapour/laser light sheet technique was conducted.
During the flow visualizadon, the laser light screen did not pulsate: a pulsating laser light screen was applied in the low speed test (Ref. 1). In the present test a continuous laser light screen is used. Recordings were made by an Intensified High Speed Video camera (MSV, see section 2.5), with a possible recording frequency of 1000 Hz. Due to the short exposure time, necessary for a sharp recording during the pitch motion *of the* model the amount of light was to small for a normal recording; therefore the camera had a special feature to intensify the amount of light. The start of recording with the IHSV is controlled by the same signal generator which provides the signal for the hydraulics to oppose the model motion. In this way perfect synchronization of the flow visualization with

model motion is achieved. During registration, 1092 pictures were recorded in the memory of the IHSV system with a frame rate of 16 pictures per cycle of the model motion. The size of the frames recorded such are 239 x 192 pixels. An illustration of this principle is given in figure 6a. Because of the synchronization of the start of recording at a zero passage of the upstroke of the model all frames have identification of the actual phase angle and flow condition. After recording, the next case (e.g. the next amplitude of the model) is adjusted, while a selection of pictures is dumped to a VHS analog video tape. Because resolution is lost in this operation another (smaller) selection of frames is dumped for storage in binary files on the computer. In this way for each test condition a selection of frames was preserved without loss of resolution.

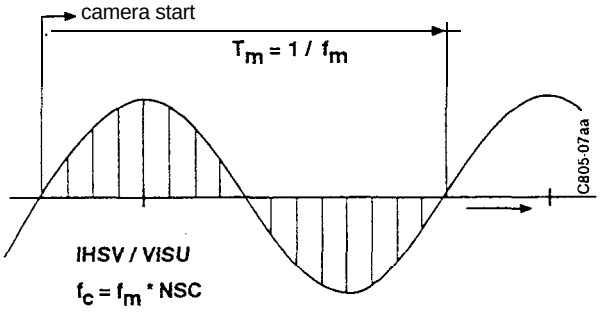


Figure 6a: Principle of MSV recording

## 3.3 Particle Image Velocimetry Testing

Quantification of flow field phenomena as observed with the vapour screen flow visualization technique is limited to "major" phenomena such as vortex and shock positions, but not to velocities and direction of local flow. For the quantification of the latter phenomena another technique is applicable, called Particle Image Velocimetry. To investigate the possibilities of PIV for the UTDP a demonstration was set up.

PIV is a technique for determining two out of three components of the instantaneous velocity field in the flow by measuring the displacement of tracer particles in the flow in a small time interval. This is achieved by multiple (i.e. double) illumination and recording of the tracer particles in a plane in the flow. NLR has developed a PIV system for use in its wind tunnels consisting of a laser light sheet system, a digital recording system and a seeding system.

The laser light sheet system consists of a double pulse Nd:YAC laser, capable of firing two high energy laser pulses with a frequency of 10 or 30 Hz. at any desired time delay between the two pulses in the order of 100 nanoseconds to micro-seconds, high reflective mirrors, to guide the laser beam to the desired location and special coated optics to form the laser light sheet.

With this system a thin sheet of the flow can be illuminated twice in a short time interval. The tracer particles in the light sheet will scatter the laser light, that can be recorded by the digital recording system. This system consists of a 1008 x 1018 pixels CCD camera, capable of recording two full frame images within 1 microsecond. The camera's digital output (1024 x 1024 pixels) is read into a Personal Computer, equipped with a fast digital signal processor board with digital interface for connection to the CCD camera. The system is capable of reading 30 images/second, when the laser is firing double pulses at a repetition frequency of 10 Hz. The recording speed was 20 images/second, storing each laser pulse information in a separate image.

The recorded images are processed using dedicated software, making correlations between data of each photograph. In that way quantified flow field information can be obtained, when information on test conditions and test setup is available.

During the PIV demonstration a laser light sheet was generated at a fixed model position in a chordwise section near the tip, so in the direction of the flow. The oil smoke, nebulized oil or water vapour particles were registrated by the High Reolution Camera (HRC).

The principle of the PIV registration technique is illustrated in figure 6b. The memory of the camera was such that 12 frames could be registered before dumping the data. During the PIV demonstration the model was not vibrating in pitch.

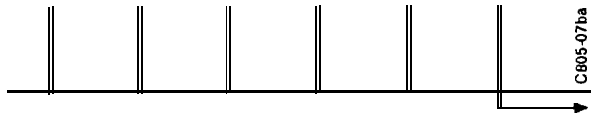


HAC / PIV

$f_c$ = 10 Hz. double pulse

Pulse duration adjustable
memory 12 frames (1024 x 1024)

Figure 6b: Principle of PIV recording

## 4 Test Program

Because this flow-visualization wind tunnel test had to provide results to complement the high speed force and pressure data base from the earlier LCO and Simple Strake tests. Main targets were:

- to identify flow field characteristics for conditions typical of transonic Limit Cycle Oscillations, mainly occurring at low incidences below 12°,
- to identify flow field characteristics for conditions dominated by vortex, shock/vortex interactions and separated flows, mainly at high incidences above 12" up to post stall, and
- to determine temporal and spatial properties of these characteristics in both incidence ranges.

Because the effects governing typical transonic LCO were expected to act especially on the outboard region

of the wing it was decided to use the Simple Strake model, with the possibility to connect various launcher and launcher/missile combinations at the tip station. The various configurations of the model during this visualization test are presented in figure 7.
Indicated are the sections were flow visualization was performed. Sections 1 to 7 have the same location as the pressure sections during the Simple Strake experiment; in the LCO experiment the same pressure sections were present but the outboard wing was at another position because of the difference in fuselage.

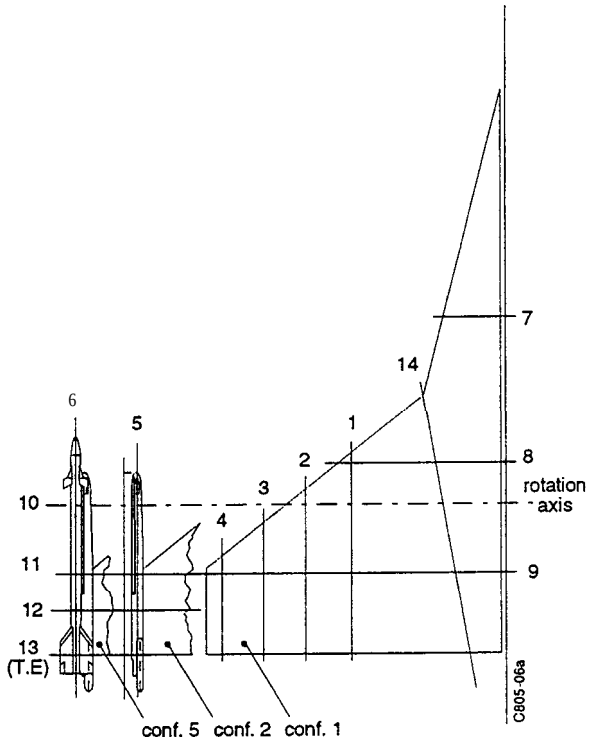


Figure 7: Sheet positions and configurations

4.1 LCO Condition Flow Visualization

For LCO investigations it was repeatedly shown that a very fine resolution in Mach number and incidence is very important (see Ref. 7). In the LCO test, configurations with different weapon loadings and flap settings were tested with half a degree increment of the mean incidence and 0.015 increment in Mach number, especially in the region of alpha-Mach combinations where LCO was observed during flight tests.
In the visualization test on the simple suaked wing conditions where wind tunnel LCO was expected to occur were looked for. This was done with and without selected tip stores (figure 7, configurations 1,2 and 5). Selected Mach numbers were M = 0.85 and M = 0.90 at incidences varying between **a =** 7" and a = 11°. For the LCO condition flow visualization typical light sheet positions were i) the mid tip chord position and ii) the trailing edge position (figure 7, sheets 11 and 13).

Interesting conditions were looked for using the normal video, recording sweeps in the incidence range of interest. Analysis of the recordings lead to the detection of typical conditions, which were measured and recorded in detail with the IHSV camera.

4.2 High Incidence Flow Visualization

The high incidence flow visualization on the Simple Strake configuration was tested at various Mach numbers. All Mach numbers were tested at a Reynolds number (based on the root chord) of 8.0 * $10^6$.
At M = 0.9 incidence sweeps ranging from a = 1" up to a = 36" were recorded with the normal speed video side camera. This was done at sheet positions 1 and 3. By controlling the oscillator at a low frequency (1 Hz., da = 0°) and triggering at a low frame rate of 8 frames per cycle it was possible to use the Intensified High Speed Video camera for recording instantaneous incidence sweeps of the model. At M = 0.6 sweeps from $a$ = 6" up to a = 36° were recorded at spanwise sheet position 9 , and for M = 0.9 at spanwise sheet positions 8 and 9 (figure 7). During these sweeps no balance measurements were performed. From these sweep recordings a selection of conditions was made to perform unsteady measurements.

4.3 Particle Image Velocimetry Demonstration

To familiarize with seeding, triggering and the complete Particle Image Velocimetry setup the demonstration was started at a low Mach number, M = 0.225. For this Mach number and for M = 0.600 PIV recordings were made for incidences of 12, 14, 16, 18 and 20 degrees. Nebulized oil particles or oil smoke particles were used as seeding. As was mentioned earlier the laser light sheet postion was fixed at location 3 (see figure 7). Corresponding force and pressure data can be returned from the Simple Strake wind tunnel test.
It was also tried to do some PIV measurements and calculations at M = 0.900 both with nebulized oil as with water vapour, as in the visualization setup. PIV calculation techniques were not successful1 at this Mach number, neither for oil particle seeding, nor for water vapour seeding. However, water vapour in combination with the pulse laser and high resolution camera turned out to be an excellent way to perform flow visualization.

## 5 Presentation and Explanation of Results

5.1 Vapour Screen Flow Visualization Data

In figure 8 an example is given of the results of *the* vapour screen flow visualization technique. For the presented situation at M = 0.85, $a$ = 9°, $da$ = 0.5". f = 40 Hz. at sheet postion 13 (Fig.7), a full recording of 1092 frames was made in memory in digital form

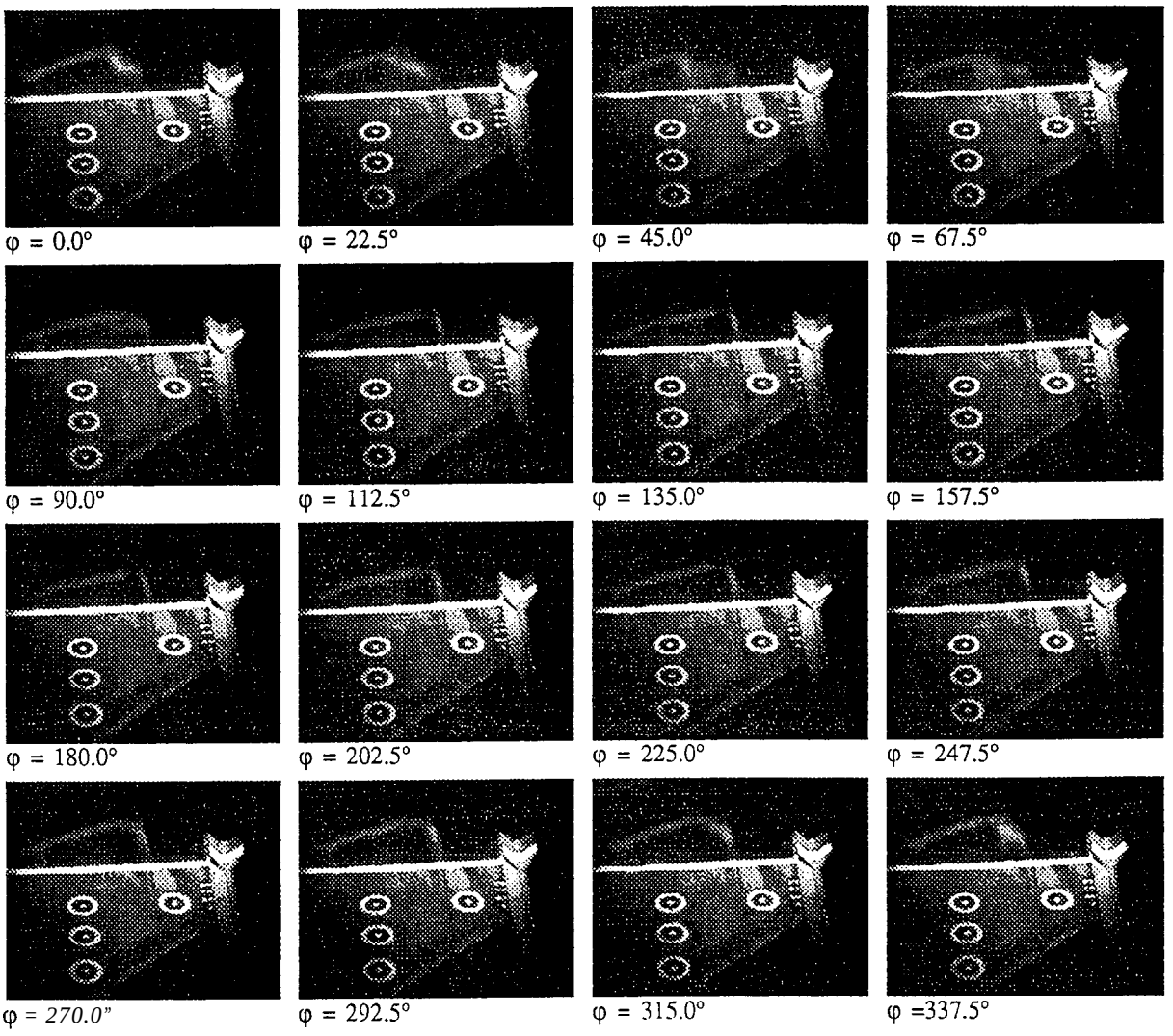


Figure 8: IHSV recordings of configuration 5 at M = 0.85, $\alpha$ = 9°, $d\alpha$ = 0.5°, f = 40 Hz., sheet 13

of the IHSV as described in section 2.5, with the setup as shown in figure 4.
A selection of these frames was stored on normal analog VHS video tape and an even smaller selection was stored digitally on computer.
Figure 8 shows a selection of frames, no. 273 up to 289, out of the full recording of 1092 frames. The graphs visualize the outboard region of the Simple Strake configuration with an additional tip launcher/tip missile combination with the viewer standing upstream of the model and looking downstream in flow direction. Due to the synchronization of model motion and camera triggering it was possible to register the flow phenomena in one complete cycle at phase angles intervals of 22.5".
Unfortunately the strake vortex is just inboard the region covered by the IHSV recording. What can be seen on the set of recordings is a sheer layer terminated by a (forward) shock. This sheer layer is produced by the forward shock and the strake vortex cross flow shock. The shock is stable during most of the cycle between phase angles φ = 90° and φ = 315°, but in the upstroke of the model motion shock induced (trailing edge) separation occurs and the shock moves inboard.

## 5.2 Particle Image Velocimetry Data

An example of what the Particle Image Velocimetry technique is capable of is given in figure 9a through 9c. This is a PIV recording at M = 0.225 and $\alpha$ = 20" on the clean model (streamwise sheet position 3 in figure 7). As explained earlier a double photograph of the flow field at times with a very short interval are taken. The first of these photographs is presented in figure 9a and the second in figure 9b.
In the lower left corner of these figures part of the model is visible. The Leading Edge is at the left margin of the figures. Although the model was completely black reflections on the model were present. The separated flow, originating at the leading edge is vaguely visible. Because there were two

imperfections in the PIV setup these photographs differ. The first imperfection is that the amount of energy in the laser light pulses was not the same. The amount of energy in a pulse is a condition that can be adjusted and an optimum has to be found. The second imperfection is that the exposure time of the two photograph is not exactly the same. The exposure of the second photograph is always a fraction longer, resulting in more visibility of background light and reflections. It is tried to adjust both features as well as possible.
These imperfections lead, apart from the changed flow field, to the difference in pictures. The larger amount of background light is clearly visible in the upper left comer of figure 9b in comparison to figure 9a. Phenomena in the flow field can be observed in both figures regardless of the short exposure times.
The positions of the (seeding) particles in both photographs can be correlated. The result of such a PIV correlation calculation based on figures 9a and 9b is shown in a so called vectorplot in figure 9c. Both frames have a size of 1024 x 1024 pixels. In the calculation a number of parameters can be defined such as:

- working area;
  area which has to be investigated in the PIV calculation; this does not have to be the total area,
- averaging area (e.g. 64 x 64 pixels);
  area defined to correlate all particles in the area and average out to one vector in that area.
- number of areas per direction (e.g. 50);
  by combining working area and averaging area an offset is calculated for the vector calculation of the next averaging area; in this way overlap of averaging areas is possible.

Due to the time interval between the frames, and the movement of the flow some particles are present in one frame and not in the other: therefore correlations are hard to make and vectors appear in the vector plot that can obviously not be possible. Vector errors also occur in areas were reflections are present. These vectors have to be smoothed out. This can be seen in figure 9c in the upper left corner (background reflection), in the lower left comer (model reflection) and on the right side of the figure (presence only in first frame, no correlation possible).
The Leading Edge separation, which is vaguely visible in figures 9a and 9b, is present in the lower part of the vector plot. The direction of the arrows corresponds to the direction of the flow; the length is an indication for the local velocity in the **flow.**

## 5.3 Pulse Laser Flow Visualization Data

As was mentioned in section 4.3 PIV calculation techniques were not successful1 at M = 0.90, neither for oil particle seeding, nor for water vapour seeding. However. water vapour in combination with the pulse laser and high resolution camera turned out to be an excellent way to perform flow visualization.

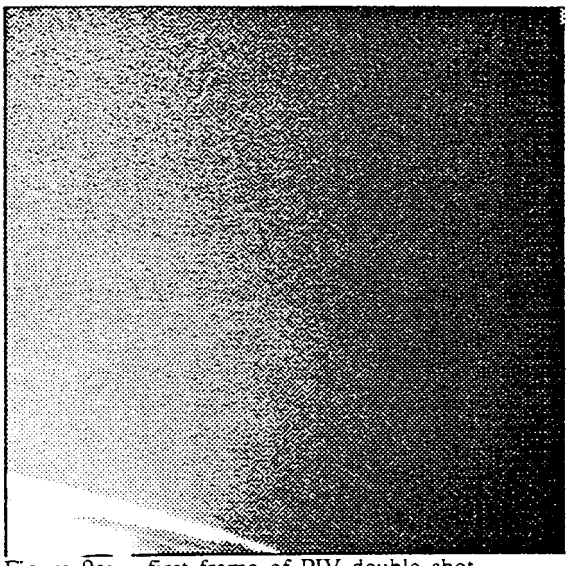
Figure 9a: first frame of PIV double shot

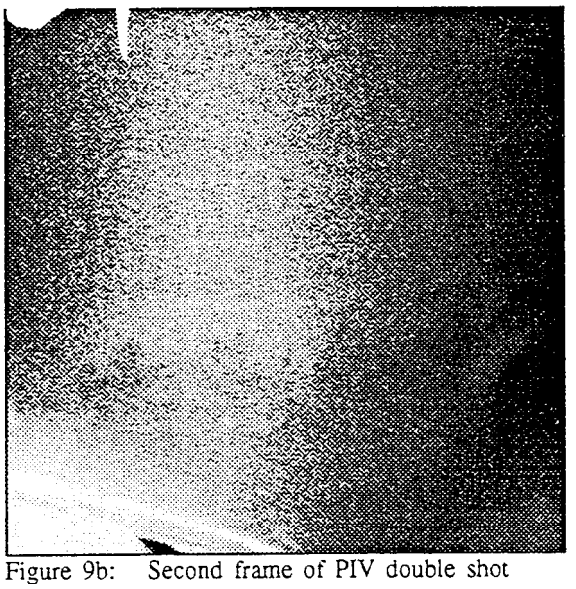
Figure 9b: Second frame of PIV double shot

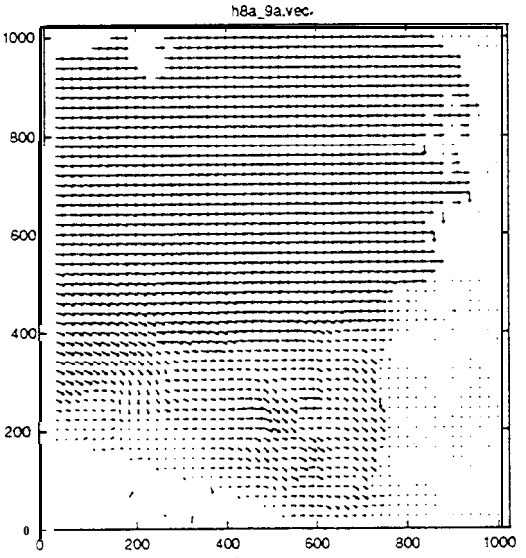

Figure 9c: PIV vectorplot

The advantages of visualizing the flow with the pulse laser and the high resolution camera in comparison to the vapour screen flow visualization technique as explained in section 3 are:

- more information (1024 x 1024 pixels vs. 239 x 192 pixels),
- better illumination of the particles (pulse laser vs. continuous laser) and therefore more detailed pictures.

The main disadvantage of the method of pulse laser visualization is that the memory of the High Resolution Camera is small and could only buffer 12 frames.

Examples of results of the pulse laser flow visualization method are presented in figures 10 a through c. Photographs of the clean model are shown for M = 0.90 at incidences $\alpha$ = 10.0" (Fig. 10a), a = 10.5" (Fig. 10b) and a = 11.0' (Fig. 10c) at sheet position 3. On the right side of the first graph a shock wave is clearly visible and there is no sign of shock induced separation. The presence of any trailing edge separation is not visible in this figure.

Increasing the incidence 0.5° leads to a flow situation visible in the second photograph (figure 10b); the same shock is visible, but now also separation underneath the shock is visible as dark clouds extending towards the trailing edge, moving the shock forward. Increasing the incidence again with 0.5" results in a completely separated flow, starting at the leading edge.

Flying at conditions of figure 10a a small disturbence can generate shock induced trailing edge separation on (part of) the wing. Higher suction will occur on the rear part of the upper surface, resulting in a nose down moment of the section. With increasing incidence leading edge separation causes loss of suction pressures at the front part of the section, resulting in a nose-up contribution to the sectional pitching moment. This change in aerodynamic moment forces a decrease in incidence felt by the section and has a stabilizing effect on the flow. Flying at an incidence where these phenomena originate can result in a kind of "flip-flop" movement which is believed to be the driving mechanism for Limit Cycle Oscillations. For more information on this subject see reference 8.

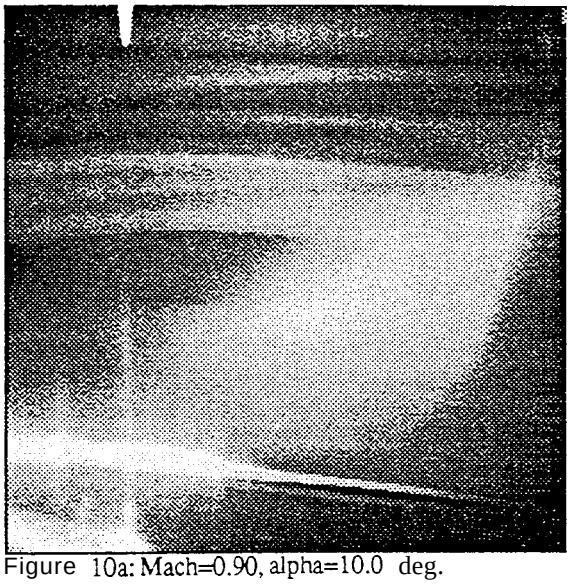

Figure 10a: Mach=0.90, alpha=10.0 deg.

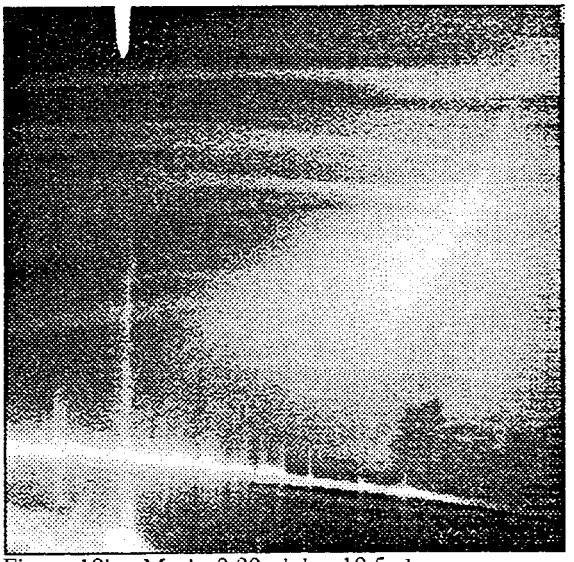

Figure 10b: Mach=0.90, alpha=10.5 deg.

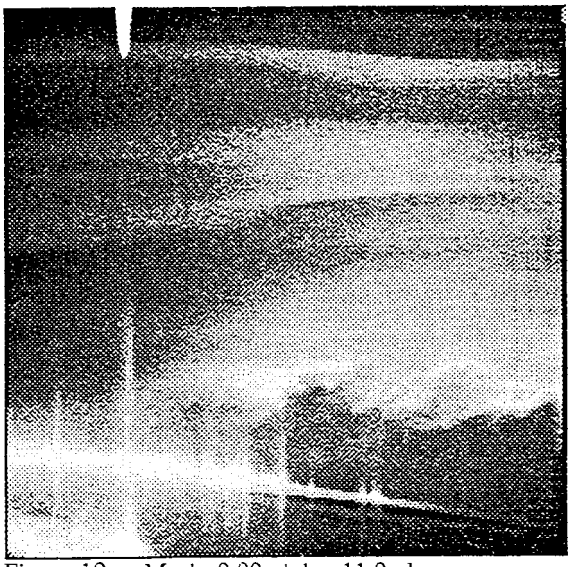

Figure 10c: Mach=0.90, alpha=11.0 deg.

## 6 Final Comment and Concluding Remarks

The flow visualization test using the vapour screen technique, has provided useful spatial information about shock wave and vortex sheet locations.

Correlating the earlier results from LCO-test and Simple Strake test with the visualization test results will increase the knowledge and understanding of flow field characteristics for conditions typical of transonic Limit Cycle Oscillations and high incidence vortex flows.

The insight in the temporal and spatial properties of the flow characteristics will help to better develop the LCO prediction method.

Particle Image Velocimetry is demonstrated to be a technique applicable for quantifying visualized flow field information in stationary conditions. If data transport can be improved unsteady PIV will be possible in the near future.
However, improvements have to be made regarding traversability of light sheet positioning and camera positioning for a wider use.

The pulse laser flow visualization has shown promising results.

## 7 Acknowledgement

The author wishes to thank Ir. R.J.W. den Boer for his help in preparing the PIV pictures and calculations and for the fruitful1 discussions on the phenomena related to PIV, concerning this paper.

## 8 References

1. Cunningham, Jr., A.M., den Boer, R.G., et al, "Unsteady Low-Speed Wind Tunnel Test of a Straked Delta Wing, Oscillating in Pitch", AFWAL-TR-87-3098 (Parts I through VI), 1988.

2. Cunningham, Jr., A.M., den Boer, R.G., "Transonic Wind Tunnel Investigation of Limit Cycle Oscillations on Fighter Type Wings", AGARD SMP Specialist Meeting on Transonic Unsteady Aerodynamics and Aeroelasticity, San Diego, California, 9-11 October 1991.

3. Cunningham, Jr., A.M., den Boer, R.G., "Transonic Wind Tunnel Investigation of Limit Cycle Oscillations on Fighter Type Wings - Update", 33rd AIAA, ASME, ASCE, AHS, ASC, SDM Conference, Dallas, Texas, April 13-17, 1992.

4. Cunningham, Jr., AM., den Boer, R.G., Dogger, C.S.G., Geurts, E.G.M., Retèl, A.P., Zwaan, R.J., "Unsteady Transonic Wind Tunnel Test on a Semi-Span Straked Delta, Wing Model Oscillating in Pitch", NLR CR 93570 L (Parts I through III), 1993.

5. Meijer, JJ., Cunningham, Jr., A.M., "A Prediction Method of Transonic Limit Cycle Oscillation Characteristics of Fighter Aircraft using Adapted Steady Wind Tunnel Data", 19th ICAS Congress, Anaheim, California, September 18-23, 1994.

6. Meijer, J-T., Cunningham, Jr., A.M., "Outline and Applications of a Semi-Empirical Method for Predicting Transonic Limit Cycle Oscillation Characteristics of Fighter Aircraft", International Forum on Aeroelasticity and Structural Dynamics 1995, Manchester, UK, 26-28 June, 1995.

7. Elbers, W.K., "Wind Tunnel Data Report 1/9 Scale F-16A Pressure Model Investigation of Shock Induced Separation for Limit Cycle Oscillation Studies (AEDC PWT-16T Test TF-695)", General Dynamics, Fort Worth Division Report 16PR4694, September 1985, (Contract No. F33657-84-C-2034).

8. Geurts, E.G.M., "Presentation and analysis of results of an unsteady transonic wind tunnel tesf on a semi-span delta wing model, oscillating in pitch", International Forum on Aeroelasticity and Structural Dynamics 1995, Manchester, UK, 26-28 June, 1995.